CHAPTER V

SURFACE ENHANCED RAMAN SCATTERING OF 2-BROMO-3-METHYLAMINO-1,4-NAPHTHOQUINONE (BMANQ) BY Ag NPs

Abstract

SERS technique has been employed to investigate the orientation of 2-bromo-3-methylamino-1,4-naphthoquinone (BMANQ) molecule on Ag NPs. Ag NPs have been prepared by solution combustion method with citric acid as fuel. The observed intense C=O stretching, C–Br stretching, in-plane of C-H mode and NH_2 vibration suggests that the BMANQ molecule may be adsorbed in a 'stand-on' orientation to the Ag NPs. The calculated highest occupied molecular orbital (HOMO) and lowest unoccupied molecular orbital (LUMO) energy show that charge transfer occurs within the molecule.

5.1 Introduction

Naphthoquinone (NQ) is the most important derivatives of naphthalene. They are of significant interest in chemical and biochemical fields. Naphthoquinone has been widely used in various fields such as dye for cosmetics, textiles, foods, and for curative purposes, including antiphthisic, antitumor, anti-inflammatory, antimicrobial agents, and antimalarial action and can be used for pharmacological treatment of different types of respiratory diseases, especially cancer [1-3]. In this present investigation, SERS spectral analysis of BMANQ molecule on Ag NPs and the analysis of vibrational modes observed both in experimental and computational method were studied. HOMO-LUMO analysis of BMANQ molecule and BMANQ molecule with Ag NPs were also investigated.

5.2 Experimental

5.2.1 Materials

The details of the chemicals used are similar as discussed in chapter III. BMANQ molecule was synthesized according to the literature [4].

5.2.2 Synthesis of Ag NPs using solution combustion method

Ag NPs used in this study were synthesized by solution combustion method as discussed in chapter II and III.

5.2.3 Characterization

The details of the instruments used are similar as described in chapter III.

5.3 Result and discussion

5.3.1 HOMO-LUMO studies

The HOMO and LUMO are the main orbital take part in chemical stability. The HOMO represents the ability to donate an electron and LUMO as an electron acceptor. The HOMO and LUMO energy gap calculated by DFT/B3PWY method. The electronic transition absorption corresponds to the transition from the ground to the first excited state and is mainly described by an electron excitation from the HOMO to LUMO. Analyzing the structures of molecular orbitals in the ground state and excited state can help us identify the binding sites of specific electrophilic and nucleophilic adsorbates. The qualitative approach of molecular orbital analysis uses a molecular orbital diagram to visualize bonding interaction in a molecule. The smaller

the energy gap, the greater is the reactivity [5]. The frontier molecular orbitals of title molecule are shown in figure 5.1 (a) and (b) In the molecular orbital diagram, the positive phase is shown in red and the negative is shown in green colour. The energy gap of HOMO–LUMO explains the eventual charge transfer interaction within the molecule, which influences the biological activity of the molecule. The energy gap of the title molecule was calculated at DFT/B3PWY level, which reveals the chemical reactivity of BMANQ molecule and establishes the occurrence of eventual charge transfer within BMANQ molecule. The calculated HOMO and LUMO energies are HOMO energy = 6.08eV and LUMO energy = 4.71eV. HOMO–LUMO energy gap =1.37eV. The chemical hardness and softness of a molecules having small energy gap are more polarizable because they need small energy for excitation. Due to the chemisorptions of the BMANQ molecule with the Ag NPs, the molecular orbital of the donor molecules are mixed with metallic band states. Definite orbital of donor molecules interact strongly with the acceptor molecules and are responsible for the chemisorptions bonds. The HOMO and LUMO (figure 5.1 (b)) of BMANQ molecule on Ag shows the molecular orbitals, in which the HOMO surface is well localized within the Ag. This result in significant excited state Donor–Acceptor mixing and the appearance of charge transfer band in the electron adsorption spectrum. By comparing both cases, energy band gap between HOMO–LUMO of Donor–Acceptor mixing (0.727eV) is lower than that of donor molecule (1.37eV) which indicates to strong intermolecular interaction. Moreover, the lower HOMO and LUMO energy gap explains the eventual charge transfer interaction taking place within the molecule which is responsible for the chemical activity of the molecule.

5.3.2 *SERS studies*

5.3.2.1 Vibrational assignments

The structure of BMANQ molecule is shown in figure 5.2. The normal Raman (nRs) and SERS spectrum of BMANQ are shown in figure 5.3 and 5.4. The wavenumber of the observed Raman and SERS bands, their relative intensities and the assignments are given in table 5.1.

The C-C stretching (ring stretching) vibrations are very important in the spectrum of naphthalene derivatives and are highly characteristic of the aromatic ring itself. Naphthalene ring C-C stretching vibrations are expected in the region 1600-1250cm^{-1} and these vibrations are found to make a major contribution in the Raman and SERS Spectra [6]. In this view, the C-C aromatic stretches are observed at

1630-1336cm^{-1} in the nRs and the strong peaks are observed at 1649-1330cm^{-1} in the SERS spectrum. The C-C stretching vibration, were assigned to coupled vibration of N-H bending and CH_3 deformation vibrations.

The C-H in-plane bending vibration usually occurs in the region 1300-1000cm^{-1} and is very useful for characterization purposes [7]. In the present case, C-H in-plane bending vibrational modes are observed in the region 1284-975cm^{-1} in nRs and SERS spectra in the region 1293-987cm^{-1}. The aromativity of the compound was clearly proved by the presence of strong peak below 900cm^{-1} and the substitution patterns on the ring can be evaluated from the out of plane bending of the ring C–H bond in the region 900–667cm^{-1} which are more informative [8]. In the present study, the C-H out-of-plane bending modes of BMANQ molecule occur in the region 907-665cm^{-1} in nRs and the weak and strong bands of SERS at 913-653cm^{-1} confirm the C–H out-of-plane bending vibrations which agrees well with the above said literature values [9]. The changes in the frequencies of these deformations from the values in naphthalene are almost determined exclusively by the relative position of the substituent and are almost independent of their nature.

BMANQ under consideration possesses a CH_3 group in the side-substituted chain. For the assignments of CH_3 group frequencies, one can expect that nine fundamentals can be associated with each CH_3 group, namely the symmetrical stretching in CH_3 (CH_3 symmetric stretch) and asymmetrical stretching (CH_3 asymmetric stretch) in-plane stretching modes (i.e., in-plane hydrogen stretching mode); the symmetrical (CH_3 symmetric deform) and asymmetrical (CH_3 asymmetric deform) deformation modes; the in-plane rocking (CH_3 ip), out-of-plane rocking (CH_3 op), and twisting (tCH_3) modes. Methyl groups are generally referred as electron-donating substituent in the aromatic ring system. The methyl hydrogen atoms in BMANQ are subjected simultaneously to hyper conjugation and back donation, which causes the decrease in stretching wavenumber and infrared intensities, as reported in literature [10]. The CH_3 deformation mode occurs in the region 1440-1360cm^{-1}. These assignments are also supported by the literature [11]. In the present case, nRs vibrational mode observed in the region 1451-1380cm^{-1} and 1457- 1358cm^{-1} in SERS are assigned to CH_3 deformation modes which have appeared as coupled vibrations with C-C stretching modes. The methyl rocking modes are active in the region 1070-1010cm^{-1} [12] with a band intensity which is sometimes weak, although the band can

also be of medium intensity or sometimes even be strong. In the present work, the medium intensity peak at 1080-1005cm^{-1} in nRs and 1092-1005cm^{-1} SERS spectrum are assigned to CH_3 rocking modes which appeared as coupled vibrations with C-H in-plane bending modes. The CH_3 torsion vibrational modes are observed at 186 and 115cm^{-1} in nRs and in the region 117cm^{-1} in SERS. The methyl group assignments proposed in this study is also in agreement with the literature values [13-15].

Strong characteristic adsorption due to the C-Br stretching vibration is observed with the position of the bend, being influenced by neighbouring atom or group, smaller the halide atom, greater the influence of the neighbour. Bands with weak to medium intensity are also observed for the C-Br stretching vibrations. Most aromatic C-Br stretching vibrational modes are observed strongly in the region 377 and 267cm^{-1} [7]. In the present case, a band is observed at 350-266cm^{-1} in both nRs and SERS are assigned to C-Br stretching vibration for BMANQ molecule. The C-Br in-plane bending mode is observed at 161-152cm^{-1} in both nRs and SERS spectrum.

The skeletal deformation mode of NQ molecule occurs in the region 600-250cm^{-1} [16]. The skeletal deformation mode was observed at 616-266cm^{-1} in nRs and SERS band observed in the region 619-276cm^{-1} are assigned to skeletal deformation of NQ. In NQ, ring breathing vibrational mode is observed at 690cm^{-1} [17]. The ring breathing mode was observed at 665cm^{-1} in nRs and 671cm^{-1} in SERS spectra.

The C=O stretching vibration gives rise to characteristic bands in the Raman and SERS spectra and the intensity of these bands can increase due to conjugation or the formation of hydrogen bonds [7]. Generally, the carbonyl group stretching vibration modes has been observed around 1800-1700cm^{-1} [17]. If a carbonyl group is part of a conjugated system, then the wavenumber of the carbonyl stretching vibration decreases, the reason being that the double bond character of the C=O group is less due to the π-electron conjugation being localized. For the title compound, the C=O stretching mode is seen as a strong band at 1741-1680cm^{-1} in the nRs and 1745-1686cm^{-1} in SERS spectra.

N-H bending is usually observed in the region 1650-1515cm^{-1}, which is called the amide band [18]. The N-H bending mode was observed in the region 1630-1516cm^{-1}in nRs and in SERS band are observed in the region 1649-1522cm^{-1} are assigned to N-H bending of NQ.

The band at 220cm^{-1} is due to the stretching mode between metal and adsorbate. In most of the study on nitrogen heterocycles adsorbed on silver electrodes, this line is recognized to the weak Ag-N bond [19]. In the present case, the nRs band at 211cm^{-1} and SERS band observed at 220cm^{-1}was assigned as Ag-N stretching vibrational mode.

5.3.2.2 Orientation of BMANQ molecule and BMANQ molecule on Ag NPs.

The surface enhancement depends on the following factors. The first effect is the kind of adsorption between chemical compound and metal nanoparticles, i.e. chemisorptions or physisorption. Chemisorptions shows high surface enhancement when contrasted to physisorption. The second effect depends on the orientation of the chemical compound on the metal nanoparticles i.e. flat-on or stand-on. The third effect involves the polar substitute of the chemical compound i.e. withdrawal of electron or donation of electron [20]. Molecules chemisorbed on metal surface show a larger enhancement than the physisorbed molecules, signifying some chemical effect between the molecule and the surface. It is known that the absorption coefficients of chemisorbed molecules are larger than those of strong over-layers. Some theories expect that charge oscillations between molecular orbitals and the metal surface enlarge the adsorption coefficient of adsorbates by intensity borrowed from the charge oscillations [21, 22].

Two enhancement mechanisms commonly explain SERS effect, the electromagnetic mechanism and chemical mechanism. In the electromagnetic mechanism, local electric fields in the surroundings of the metal nanoparticles were enhanced due to the surface plasmon excitation, leading to more intense electronic transition in molecules located near the nanoparticles, and enhanced Raman scattering. The electromagnetic mechanism depends on tunable optical properties of the metal nanoparticles that can be optimized in order to achieve higher SERS enhancements. The enhancement in chemical mechanism consists of increasing the molecular polarizability of the adsorbate due to the charge transfer interaction of the absorbent with metal nanoparticles surface. In the present case, the SERS enhancement in the Ag NPs was explained through electromagnetic and chemical enhancement mechanism.

There are two possible orientations that the molecule that may adsorb through chemisorptions process, i.e. ‘face-on’ and ‘stand-on’. The BMANQ molecule has three binding sites, i.e. aromatic ring, long pair of electron of the nitrogen and carbonyl groups. These features may lead to the adsorption of the molecule on the Ag NPs [23]. The orientation of the molecule on the Ag NPs can be inferred from aromatic C-C stretching, ring breathing, in-plane bending, out-of-plane bending, and the SERS surface selection rule.

The possible ring breathing mode represents sufficient information of the orientation in NQ. The ring breathing mode of SERS that occurs at 671cm^{-1} was upshifted by about 6cm^{-1} and the bandwidth was decreased, compared to 665cm^{-1} for nRs. In the SERS spectra, the metal-molecule interactions increase the frequency of the ring breathing mode when compared to the ‘free’ molecule in the solid state. It was clearly proposed that BMANQ molecule adsorbed on the Ag NPs in a ‘stand-on’ orientation.

Generally, quinone derivatives are adsorbed on the metal nanoparticles through the C=O binding site. One more promising way in which the BMANQ molecule ‘stand-on’ adsorption occurs on the Ag NPs is through the C=O. Carboxylate group can interact strongly with metal through the formation of charge transfer compound between adsorbed and metal nanoparticles, where adsorbate operates like a donor and the metal as acceptor. The intensity of the peak increases and the wavenumber is downshifted with respect to the corresponding nRs band [24]. In the present case, bands are observed in region 1741,1711 and 1680cm^{-1} in nRs and SERS bands are observed in the region 1745,1721 and 1686cm^{-1} of BMANQ molecule on Ag NPs due to C=O stretching. The observed peak intensity and upshifted wavenumber of C=O stretching mode indicates that the molecule is adsorbed on the metal through C=O stretching. In addition, the vibrations relating to atoms that are close to the Ag NPs will be enhanced. When the wavenumber difference between nRs and SERS spectra is not more than 10cm^{-1}, the molecular plane will be perpendicular to the Ag NPs [24]. In the present case the difference between nRs and SERS not more than 10cm^{-1} wavenumber for C=O stretching which also evidence that the BMANQ has ‘stand-on’ orientations.

The strength of out-of-plane vibrational modes decreases substantially relative to the in-plane vibrational modes, when the adsorbed orientation is distorted from parallel to 'stand-on' orientation. The high intensity of in-plane vibrational modes occurs in the region 1293-987cm^{-1} in SERS and nRs vibrational modes occur in the region 1284-975cm^{-1}. The C-H out-of-plane vibrational modes were observed in the region 913-653cm^{-1}in both nRs and SERS. In our case, the intensity of in-plane vibrational modes has increased with respect to the out-of-plane bending mode. This once again confirms the 'stand-on' orientation of BMANQ adsorbed on Ag NPs [25]. When the molecules adsorbed 'stand-on' the Ag NPs, the polarizability tensor corresponding to out-of-plane vibration was parallel to the metal surface. Some of the out-of-plane vibrational modes are not observed in the SERS spectrum. The intensity of the peak at 907, 854, 758, 724 and 665cm^{-1} in nRs is less than that of the peak at 913, 857, 764, 727 and 671cm^{-1} in SERS also indicates that the greater possibility of the 'stand-on' orientation of BMANQ molecule adsorbed on Ag NPs.

The C-C stretching vibrations are generally most important in the spectrum of NQ and its derivatives are characteristic of aromatic ring. C-C ring stretching vibration modes usually occur in the region 1600-1250cm^{-1} [6]. The nRs wavenumber of C-C stretching vibrational modes have decreased by greater than 10cm^{-1} and their bandwidth increases considerably when the molecule adsorbs on the metal nanoparticles via their π system. The nRs and SERS shows that sixteen ring stretching vibration mode occur in the region 1649-1330cm^{-1}. The bands at 1627-1330cm^{-1} in SERS are upshifted in the nRs spectrum and bandwidths are affected. But in the case of C-C stretching vibration modes the SERS modes are shifted with respected to nRs modes. In our case, the overall vibrational of C-C stretching modes increases with respect to nRs. It clearly recommends that the BMANQ molecule adsorbed on the Ag NPs in a 'stand-on' orientation. From the observed up-shifted peaks and its wavenumber, it was seen that it is difficult to make orientation of the BMANQ molecules on the Ag NPs using C-C stretching vibrations.

Another possible way in which the BMANQ molecule in a 'stand-on' adsorption occurs on the Ag NPs is through the C-Br stretching. Generally, in quinone the C-Br stretching vibrational band is very strong in intensity [26]. In the present case, bands are observed in region 350 and 266cm^{-1} in nRs and SERS bands are observed in the region 344 and 276cm^{-1} of BMANQ molecule on Ag NPs due to C-Br

stretching. The C-Br in-plane bending vibration modes also occur in the region 152 and 161cm^{-1} in nRs and SERS. In both case these modes are enhanced in SERS and shifted by 9cm^{-1}. It was evidently proposed that BMANQ molecule was adsorbed on the Ag NPs in a 'stand-on' orientation through Br.

In the present case, a new band appears at 220cm^{-1} in SERS was due to Ag-N stretching vibration mode [19]. This is indicating that the BMANQ molecule was adsorbed on the Ag NPs through the nitrogen atom in 'stand-on' orientation. The observed high SERS signal indicates that the prepared Ag NPs are good source for physical, chemical and biomedical application as SERS substrate.

From the above discussion, it is concluded that BMANQ molecules adsorb as 'stand-on' orientation on the Ag NPs through the coordinating site C=O, C-Br and NH_2.

5.4 Conclusion

Ag NPs were synthesized by solution combustion method using citric acid as fuel. The SERS spectral analysis indicates that the silver nanoparticles reveal high SERS activity. The vibrational features of C=O, C-Br and NH_2 bending modes suggest that the BMANQ molecule was adsorbed through a 'stand-on' orientation on the Ag NPs. The HOMO-LUMO analysis confirms that the energy gap value has significant influence on the intermolecular charge transfer and that the BMANQ molecule has quite established configuration.

Reference

[1] P. Rajeshwar Verma, Anti. Cancer. Agen. Med. Chem., 6 (2006) 489.

[2] O. Zakharova, L. Goryunov, N. Troshkova, Eur. J. Med. Chem., 45 (2010) 270.

[3] M. Anuratha, A. Jawahar, M. Umadevi, V.G. Sathe, P. Vanelle, T. Terme, V. Meenakumari, A. Milton Franklin Benial, Spectrochim. Acta part A., 105 (2013) 218.

[4] O. Khoumeri, M. Montana, T. Terme, P. Vanelle, P. First, Tetrahedron., 64 (2008) 11237.

[5] S.T. Aruna, A.S. Mukasyan, Curr. Opin. Solid State Mater. Sci., 12 (2008) 44.

[6] V. Balachandran, G. Santhi, Vib. Spectrosc., 52 (2012) 11425.

[7] N. R. Sheela, S. Muthu, S. Sampath Krishnan, Der. Pharma. Chemica., 4 (2012) 169.

[8] H. Kirk, M. Michaelian, M.S. Ziegler, Appl. Phys., 27 (1972) 1.

[9] N.B. Colthup, L.H. Daly, S.E. Wilberley, Intoduction to infrared and Raman spectroscopy, Academic Press, New york, (1990).

[10] M. Karabacak, M. Cinar, Z. Unal, M. Kurt, J. Mol. Struct., 982 (2010) 22.

[11] A. Altun, K. Golcuk, M. Kumru, J. Mol. Struct. (Theochem.)., 637 (2003) 155.

[12] G. Raja, K. Saravanan, K. Sivakumar, Int. J. Appl. Phys. Maths., 1 (2011) 1.

[13] D. Jagadeeswara Rao, Y. Ramakrishna1, V. Padmarao, B. Venkateswara Rao, Int. J. Adv. Res. Sci. Technol., 1 (2012) 135.

[14] J.P. Kalyani, N. Kalaiselvi, N. Muniyandi, J. Powder Sources., 111 (2002) 232.

[15] A.U. Rani, N. Sundaraganesan, M. Kurt, M. Cinar, M. Karabacak, Spectrochim. Acta A., 75 (2010) 1523.

[16] C. Sengamalai, M. Arivazhagan, K. Sampathkumar, Elixir. Comp. Chem., 56 (2013) 13291.

[17] M. Moskovits, J. Phys. Chem., 92 (1988) 6327.

[18] N. Sundaraganesan, B. Dominic Joshua, T. Radjakoumar, Ind. J. pure & appl phys., 47 (2009) 248.

[19] F.S. Parker, Kirchenbaum, Spectrochim Acta., 16 (1960) 910.

[20] B.N.J. Persson and R. Ryberg, Phys. Rev. B., 24 (1981) 6954.

[21] V. Ramakrishnan, N. Krishnamurthy, M. Gurunathan, V.J.P Srivatsavoy. Spectrochim. Acta. Part A., 46 (1990) 1615.

[22] R. Aroca, R.E. Clavijo, Spectrochim. Acta Part A., 44 (1988) 171.

[23] B. Kosar, C. Albayrak, Spectrochim. Acta A. 78 (2011) 160-167.

[24] G.Varsanyi, P. Sohar, Acta. Chim. Acad. Sci. Hung., 74 (1972) 315.

[25] K. Geetha, M. Umadevi, G.V. Sathe, R. Erenler, Spectrochim. Acta Part A., 116 (2013) 236.

[26] G. Levi, J. Patigny, J.P. Massault, J. Aubard, in: Thirteenth International Conference on Raman Spectroscopy, Wurzburg, (1992).

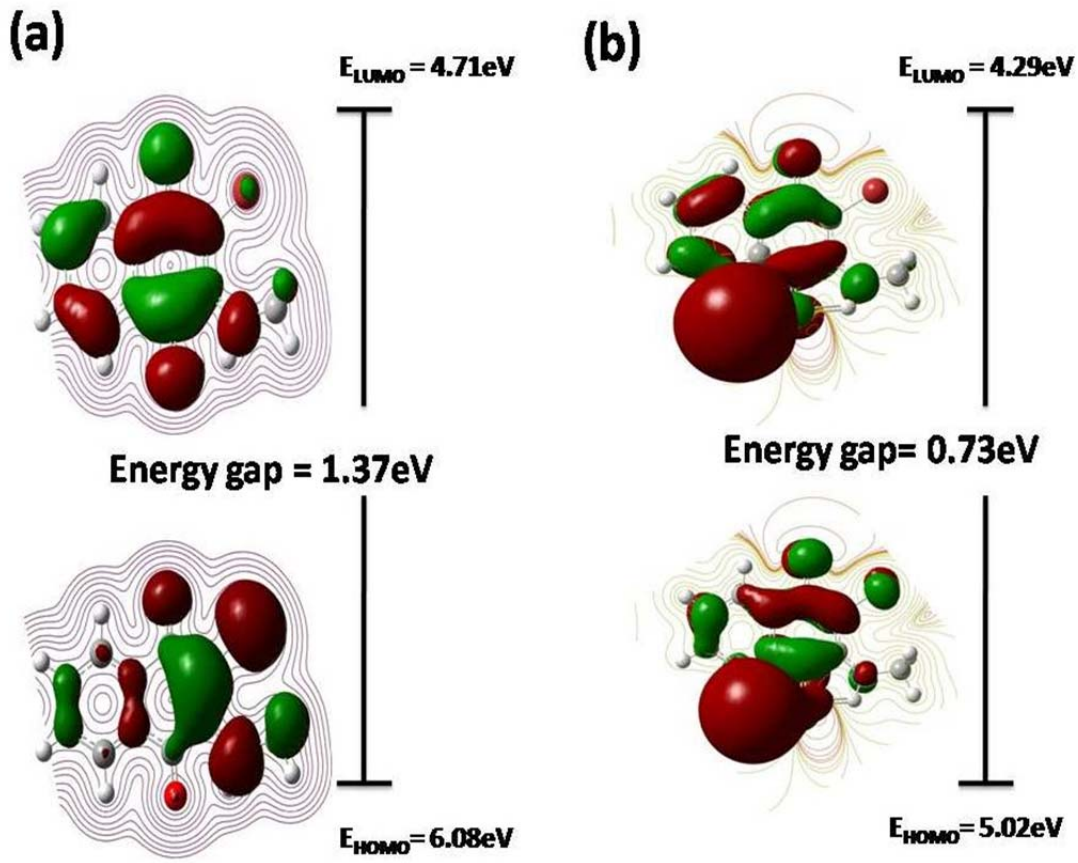

Figure 5.1 HOMO and LUMO plot of (a) BMANQ molecule and (b) BMANQ molecule on Ag NPs.

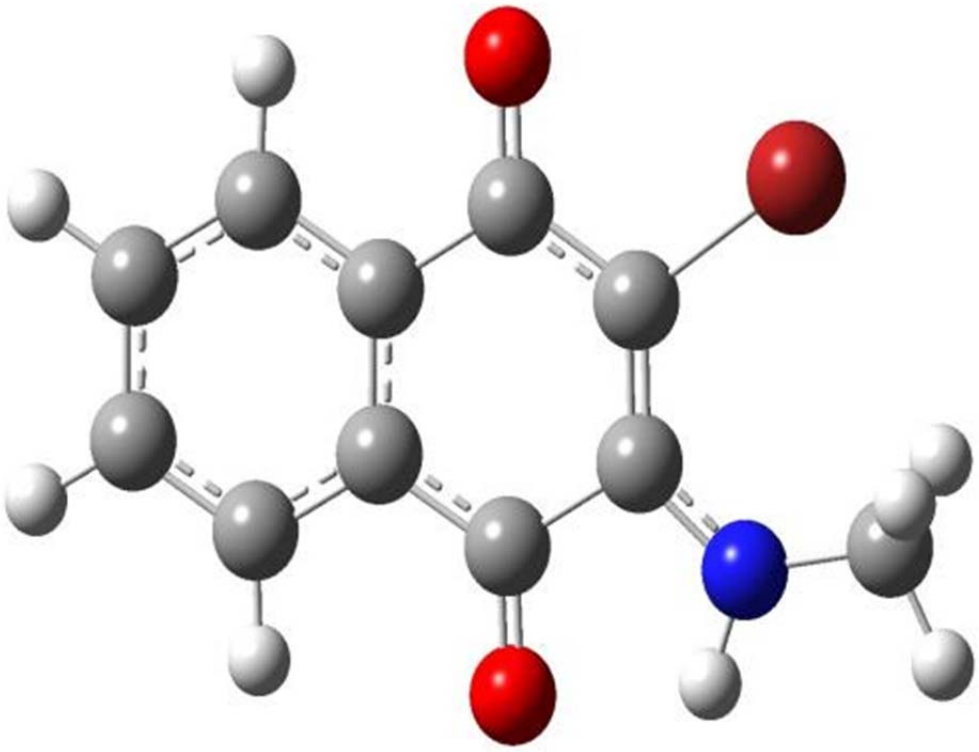

Figure 5.2 Structure of 2-bromo-3-methylamino-1,4 naphthoquinone (BMANQ).

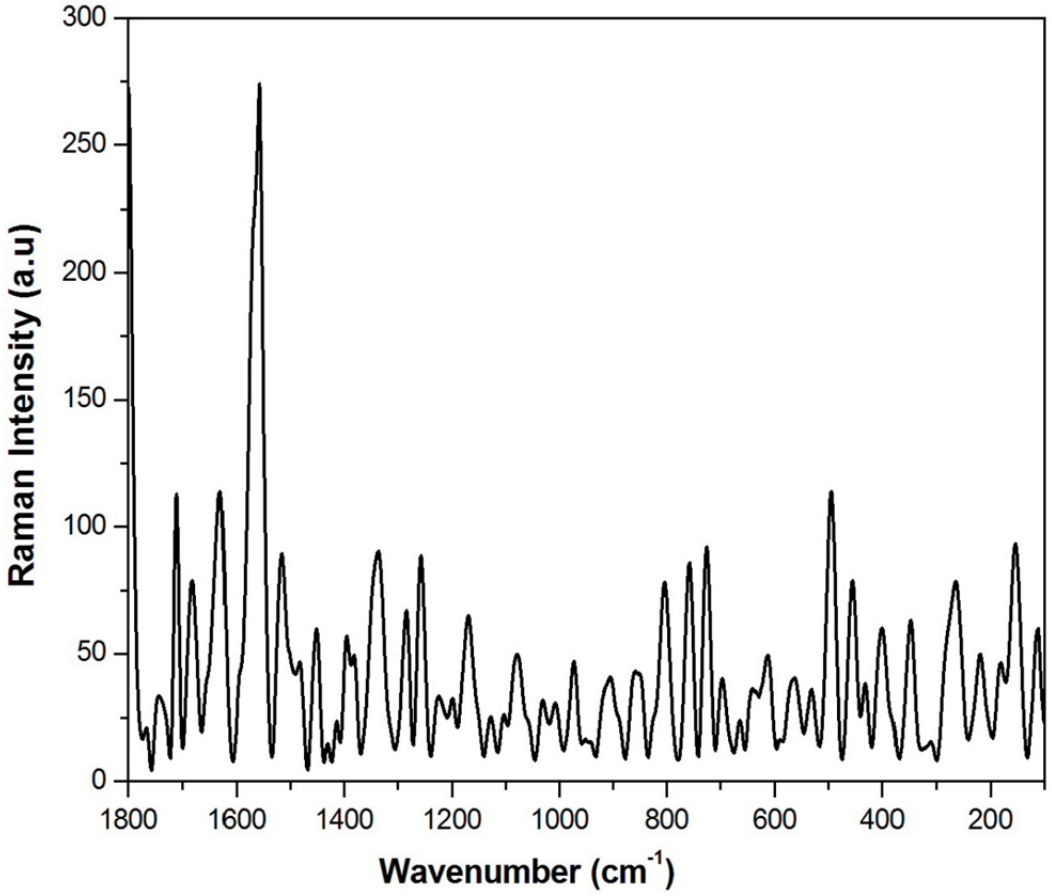

Figure 5.3 Normal Raman Spectrums (nRs) BMANQ molecule.

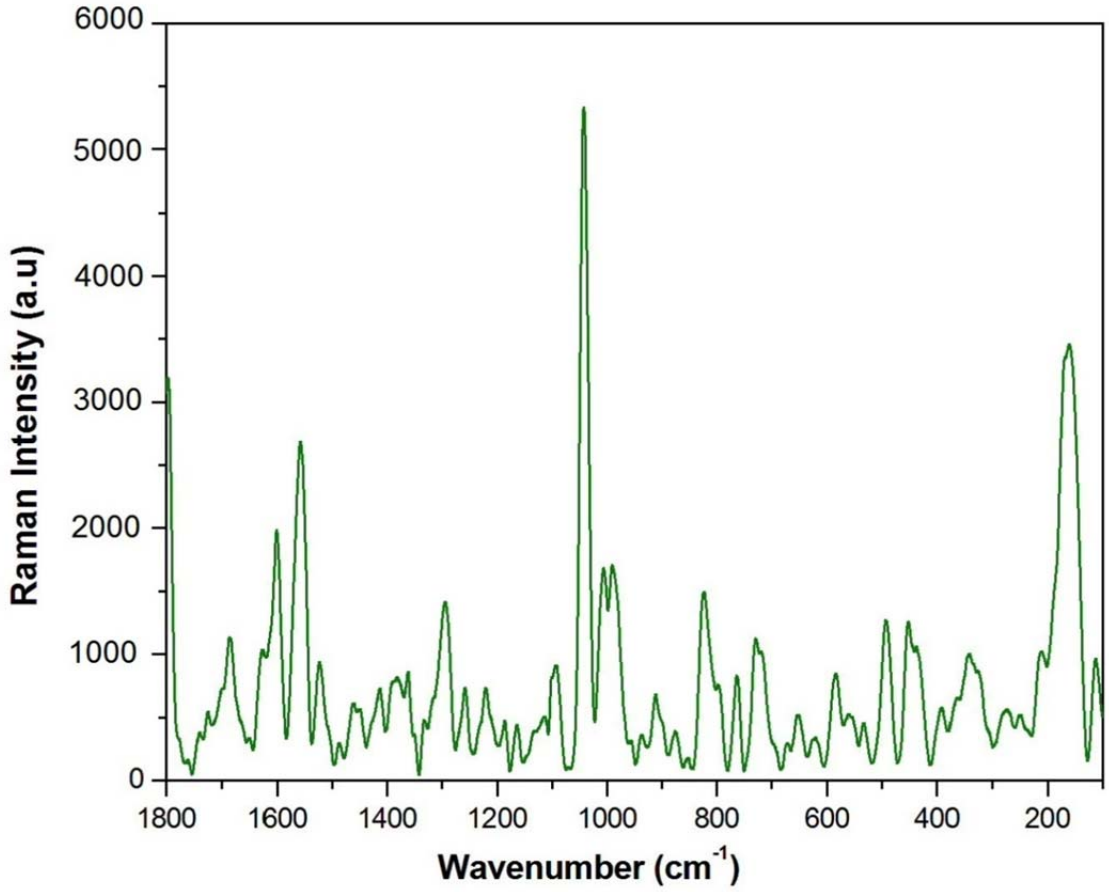

Figure 5.4 Surface Enhanced Raman spectrums (SERS) of BMANQ molecule on AgNPs.

Table 5.1 Vibrational assignment of BMANQ molecule and BMANQ molecule on Ag NPs.

Wavenumber (cm^{-1})		Vibrational Assignments
nRs	SERS	
1741	1745	C=O str.
1711	1721	C=O str.
1680	1686	C=O str.
	1649	C-C str., N-H bend.
1630	1627	C-C str., N-H bend.
		C-C str., N-H bend.
1599	1602	C-C str., N-H bend.
1553	1559	C-C str., N-H bend.
1516	1522	C-C str., N-H bend.
		C-C str.
1479	1488	C-C str.
		C-C str.
1451	1457	C-C str., CH_3 def.
1429		C-C str., CH_3 def.
1414	1417	C-C str., CH_3 def.
1395		C-C str., CH_3 def.
1380	1383	C-C str., CH_3 def.
	1358	C-C str., CH_3 def.
1336	1330	C-C str.
1284	1293	C-H i.p.
1256	1259	C-H i.p.
1200	1219	C-H i.p.
	1188	C-H i.p.
1169	1163	C-H i.p.
1126	1120	C-H i.p.
1104		C-H i.p.

1080	1092	C-H i.p., CH_3 rock.
1030	1043	C-H i.p., CH_3 rock.
1005	1005	C-H i.p., CH_3 rock.
975	987	C-H i.p.
907	913	C-H o.p.
	876	C-H o.p.
854	857	C-H o.p.
808		C-H o.p.
758	764	C-H o.p.
724	727	C-H o.p.
696		C-H o.p.
665	671	Ring breathing, C-H o.p.
	653	C-H o.p.
616	619	skel. def.
	585	skel. def.
492	492	skel. def.
455	452	skel. def.
430		skel. def.
399	393	skel. def.
350	344	C-Br str. skel. def.
266	276	C-Br str. skel. def.
211	220	Ag-N str.
186		CH_3 tor.
152	161	C-Br i.p.
115	117	CH_3 tor.

---

str. – stretching, def. – deformation, i.p. – in-plane bending, o.p. – out-of-plane bending, rock. – rocking, skel. – skeletal, as.-asymmetric, sy.-symmetric, tor.- torsion.